

## Structural Dependence of Photochromism in MEH-PPV Solutions

Magalhães, C.E.<sup>1</sup> (PG), Savedra, M.R.<sup>2</sup> (PQ), Dias, K. S.<sup>1</sup> (PG), Ramos, R.<sup>3</sup> (PQ),  
Siqueira, M.F.<sup>1</sup> (PQ)

<sup>1</sup> *Laboratory of Polymers and Electronic Properties of Materials, Department of Physics - Federal University of Ouro Preto, 35400-000, Ouro Preto – MG, Brazil*

<sup>2</sup> *Department of Chemistry, Federal University of Lavras, 37200-000, Lavras-MG, Brazil*

<sup>3</sup> *Institute of Physics, Department of Material Physics and Mechanics, University of São Paulo, 05508-090, São Paulo - SP, Brazil*

*e-mail: melissa@iceb.ufop.br*

Keywords: Photochromism, Molecular Dynamic, MEH-PPV, Organic Electronics, UV-VIS spectroscopy

### INTRODUCTION

Photochromism is a photoinduced reversible transformation of a molecular system, which undergoes to an appropriate molecular design. This phenomenon triggers changes in the optoelectronic properties of these compounds by electromagnetic radiation exposure.<sup>1,2</sup> Therefore, these kind of compound can act as electro-optical switches at molecular scale, and there is an increasing interest for applications as optoelectronic devices.<sup>3,4</sup> Previous literatures have reported the chromism effect on poly(p-phenylene vinylene) based polymers and its relationship to the structural arrangements.<sup>5,6</sup> Accordingly, these reversible molecular events can allow the development of smart materials.

The semiconducting poly[2-methoxy-5-(2'-ethylhexyloxy)-p-phenylene vinylene] (MEH-PPV), Figure 1, has been widely studied due to its electronic and mechanic properties due to its potential for applications in the field of organic electronics.<sup>7</sup> MEH-PPV can be found as red phase and blue phase, which are morphologically distinct.<sup>6,8</sup>

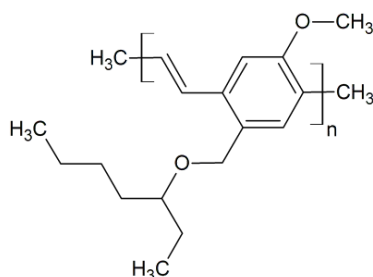


**Figure 1.** Chemical structure of MEH-PPV.

In this work, we have studied the structural arrangements of MEH-PPV in tetrahydrofuran (THF) as solvent to evaluate the photochromism behavior. To this aim, we carried out simulations using Molecular Dynamic (MD) and Quantum Mechanics (QM) approaches.

### METHODS

A MEH-PPV oligomer with nine units (nonamers) was fully optimized in vacuum using the PM6-DH+ semi-empirical calculations,<sup>9</sup> implemented in the MOPAC package.<sup>10</sup> This molecular model was used as an initial guess for modeling of the polymer solution using Molecular Dynamic simulations.

Molecular dynamic simulations were performed using the GROMACS 5.0.1 package.<sup>11</sup> The MEH-PPV and THF were modeled using the GROMOS 53a6 force field parameters.<sup>12</sup> The initial topology was built adding 20 MEH-PPV nonamers in a cubic box of 25.0 nm edge and filled with THF solvent. The PME method with 1.0 nm cutoff was used for treatment of long-range electrostatic interaction. All bonds lengths were constrained to their equilibrium values by using the LINCS algorithm. The neighbor list for the calculation of nonbonded interaction was updated every 10 time step with a cutoff of 1.0 nm, the same cutoff for Lennard-Jones potential. The PME method with 1.0 nm cutoff was used for treatment of long-range electrostatic interaction. All bonds lengths were constrained to their equilibrium values by using the LINCS algorithm. The neighbor list for the calculation of nonbonded interaction was updated every 10 time step with a cutoff of 1.0 nm.

The system was submitted to steepest descent energy minimization methodology until the maximum force attained a tolerance of  $10 \text{ kJ mol}^{-1} \text{ nm}^{-1}$ . Afterwards, from this minimized system we carried out 1.0 ns of simulation in the canonical (NVT) ensemble in order to allow the relaxing of the molecular bonds and then we carried out 1.0 ns of simulation in the isobaric-isothermal (NPT) ensemble at 300K and a small external pressure of 1 bar for 10 ns of simulation with a step size of 1 fs, using V-rescale thermostat and berendsen barostat with coupling time of  $t_\tau = 0.1 \text{ ps}$  and  $t_p = 2,0 \text{ ps}$ . The MD protocols used herein are widely employed in the literature.

The UV-VIS spectra for all final oligomer structures obtained from last frame of Molecular Dynamics were calculated by ZINDO-S/CIS method,<sup>13,14</sup> including 30 occupied to 30 unoccupied states for the single excitations. These calculations were performed with the Orca computational program, version 2.7.<sup>15</sup>

## RESULTS AND DISCUSSION

Figure 2(a) shows the initial topology of MEH-PPV:THF solution before molecular dynamic procedure. Afterward 5.0 ns of simulation we observed the clustering formation of MEH-PPV and solvent molecules, Figure 2(b). The aggregation occurs driven by the non-bonded interaction between molecules, besides temperature and solvent effects played a role into the final morphology.

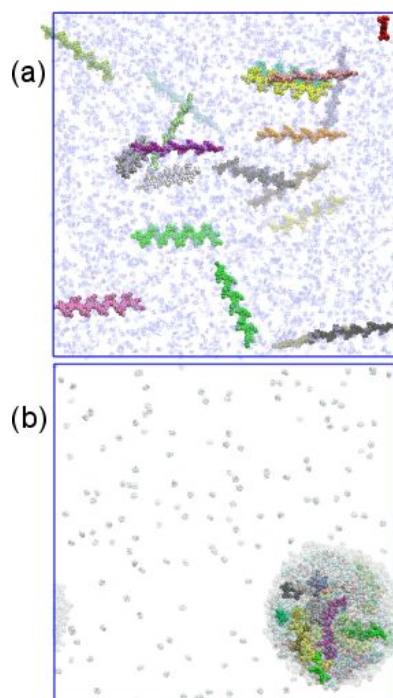


**Figure 2.** (a) Initial molecular system before the MD procedure. Box dimension with 25nm with

20 nonamers of MEH-PPV in THF as solvent. (a) Clustering formation of MEH-PPV molecules after 5.0 ns of MD simulation.

From the simulation we took two main structural arrangements found for the MEH-PPV oligomers in the solution: planar and twisted conformations. We selected two of these structures, as shown in the **Figure 3(a)** and **3(b)**. The difference between each other is the number of internal torsions which can lead to differences in the conjugation length (CL) of electronic states, being the larger CL found to the planar structure. For selected oligomers we calculate the UV-Vis spectra, presented in **Figure 3(c)**.

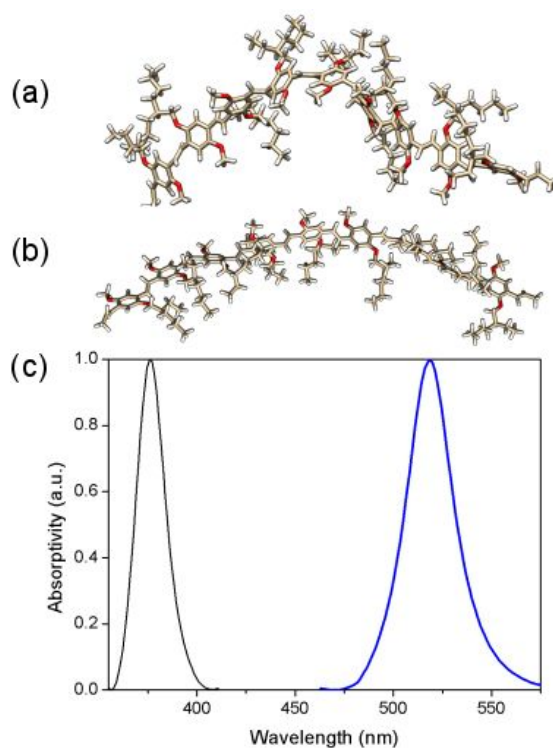


**Figure 3.** Conformational arrangements of two selected structures (a) twisted and (b) planar, from the sample after 5 ns of MD simulations. (c) Normalized first transition (HOMO-LUMO) from UV-Vis spectra calculated for these structures: in black color (for the twisted), and in blue color (for the planar); lorentzian broadening and a 11.28 half-width were added.

As it can be seen, the main electronic excitation of the twisted structure is found in the blue region. This can be directly attributed to the shorter conjugation lengths of the frontier orbitals. In the same sense, we found the main absorption transitions of the planar structure lying in the red region, which can be attributed to the larger

conjugation length for these more ordered oligomers.

Therefore, the modeling support that the difference between red and blue phases found in MEH-PPV can be attributed to intrachain electronic effects resulting from differences on the conjugation length determined by the differences in the molecular morphology.

## CONCLUSIONS

Our results support the proposal that even it would be possible to access many transient conformational arrangements under temperature effects, they will be finally converted in two main configuration: twisted and planar. Accordingly, these structural arrangements are then related to the chromism reported for these materials, the red phase is attributed to less disordered oligomers with higher electronic conjugation lengths and the blue phase is related to the shorter conjugation lengths imposed by twisted molecular morphology.

## ACKNOWLEDGMENTS

The authors thank the Brazilian funding agencies CNPq, FAPEMIG and CAPES, as well as the National Institute of Science and Technology on Organic Electronics (INEO/INCT) for financial support and fellowships.

<sup>1</sup> M. Irie, Y. Yokoyama, and T. Seki, *New Frontiers in Photochromism* (Springer Science & Business Media, 2013).

<sup>2</sup> H. Dürr and H. Bouas-Laurent, *Photochromism: Molecules and Systems: Molecules and Systems* (Gulf Professional Publishing, 2003).

<sup>3</sup> S. Masi, S. Colella, A. Listorti, V. Roiati, A. Liscio, V. Palermo, A. Rizzo, and G. Gigli, *Sci. Rep.* 5, (2015).

<sup>4</sup> J.C. Yu, J.I. Jang, B.R. Lee, G.-W. Lee, J.T. Han, and M.H. Song, *ACS Appl. Mater. Interfaces*, 6, 2067 (2014).

<sup>5</sup> E.N. Hooley, A.J. Tilley, J.M. White, K.P. Ghiggino, and T.D.M. Bell, *Phys. Chem. Chem. Phys.*, 16, 7108 (2014).

<sup>6</sup> A. Köhler, S.T. Hoffmann, and H. Bässler, *J. Am. Chem. Soc.*, 134, 11594 (2012).

<sup>7</sup> E.S. Bronze-Uhle, J.F. Borin, A. Batagin-Neto, M.C.O. Alves, and C.F.O. Graeff, *Mater. Chem. Phys.*, 132, 846 (2012).

<sup>8</sup> F.A. Feist, M.F. Zickler, and T. Basché, *Chemphyschem Eur. J. Chem. Phys. Phys. Chem.*, 12, 1499 (2011).

<sup>9</sup> J. Řezáč, J. Fanfrlík, D. Salahub, and P. Hobza, *J. Chem. Theory Comput.*, 5, 1749 (2009).

<sup>10</sup> James P. Stewart, *MOPAC* (Stewart Computational Chemistry, 2008).

<sup>11</sup> D. Van der Spoel, E. Lindahl, B. Hess, G. Groenhof, A.E. Mark, and H.J.C. Berendsen, *J. Comput. Chem.*, 26, 1701 (2005).

<sup>12</sup> C. Oostenbrink, A. Villa, A.E. Mark, and W.F. Van Gunsteren, *J. Comput. Chem.*, 25, 1656 (2004).

<sup>13</sup> M.C. Zerner, in *Rev. Comput. Chem.*, edited by K.B. Lipkowitz and D.B. Boyd (John Wiley & Sons, Inc., 1991), pp. 313–365.

<sup>14</sup> J. Ridley and M. Zerner, *Theor. Chim. Acta*, 32, 111 (1973).

<sup>15</sup> F. Neese, *Wiley Interdiscip. Rev. Comput. Mol. Sci.*, 2, 73 (2012).